Identification of a nuclear receptor/coactivator developmental signaling pathway in the nematode parasite *Strongyloides stercoralis*

Mi Cheong Cheong[a], Zhu Wang[a], Tegegn G. Jaleta[b], Xinshe Li[b], James B. Lok[b], Steven A. Kliewer[a,c,1], and David J. Mangelsdorf[a,d,1]

[a]Department of Pharmacology, University of Texas Southwestern Medical Center, Dallas, TX 75390; [b]Department of Pathobiology, School of Veterinary Medicine, University of Pennsylvania, Philadelphia, PA 19104; [c]Department of Molecular Biology, University of Texas Southwestern Medical Center, Dallas, TX 75390; and [d]HHMI, University of Texas Southwestern Medical Center, Dallas, TX 75390

Contributed by David J. Mangelsdorf, January 15, 2021 (sent for review October 21, 2020; reviewed by Adam Antebi and David D. Moore)

DAF-12 is nematode-specific nuclear receptor that has been proposed to govern development of the infectious stage of parasitic species, including *Strongyloides stercoralis*. Here, we identified a parasite-specific coactivator, called DAF-12 interacting protein-1 (DIP-1), that is required for DAF-12 ligand-dependent transcriptional activity. DIP-1 is found only in *Strongyloides* spp. and selectively interacts with DAF-12 through an atypical receptor binding motif. Using CRISPR/Cas9-directed mutagenesis, we demonstrate that DAF-12 is required for the requisite developmental arrest and the ligand-dependent reactivation of infectious *S. stercoralis* infective third-stage larvae, and that these effects require the DIP-1 coactivator. These studies reveal the existence of a distinct nuclear receptor/coactivator signaling pathway that governs parasite development.

DAF-12 | nuclear receptor | coactivator | nematode parasite | *Strongyloides stercoralis*

Parasitic nematodes are an enormous medical and economic burden worldwide (1). Despite the large number of diseases caused by these nematodes, the number of effective anthelmintic drugs is limited and resistance is an emerging problem (2, 3). To develop new drugs that target parasitic nematodes, a better understanding of the mechanisms that control the parasitic nematode life cycle is needed. Many parasitic nematodes undergo a complicated life cycle that requires several different host species to propagate, and so suitable models to study them are lacking. To circumvent this problem, *Caenorhabditis elegans* has served as a model system for parasitic nematode research because many aspects of development and gene function are conserved between *C. elegans* and parasitic species. Nevertheless, a complete understanding of the biology of parasitic nematodes and the mechanisms that are common to and differ from *C. elegans* are necessary to identify new therapeutic targets in these important pathogens.

DAF-12 is a nuclear hormone receptor initially identified in *C. elegans* (4) and is an important regulator of worm metabolism and development (4, 5). The transcriptional activity of DAF-12 is similar to that of other endocrine steroid receptors and depends on the binding of nematode-specific steroid hormones called dafachronic acids (DA) (6, 7). This endocrine signaling pathway governs a key checkpoint in the life cycle *C. elegans*, by determining whether the worm arrests its development and enters a dormant larval stage, called dauer diapause, or continuously develops to mature reproductive adults. During unfavorable conditions, the DA hormone is not produced and DAF-12 functions as a transcriptional corepressor that results in dauer diapause, permitting *C. elegans* to survive until favorable conditions return. Under favorable conditions, DA is synthesized, resulting in DAF-12–dependent expression of genes involved in promoting reproductive development and preventing dauer arrest.

DAF-12 is one of the most well-conserved signaling pathways between *C. elegans* and parasitic worms (8). The dauer stage resembles the infective third stage (iL3) of parasitic nematodes, which is specialized to seek out and infect host organisms. Orthologs of DAF-12 have been identified in all parasitic species surveyed, including hookworms, threadworms, and filarial parasitic nematodes (9–14). One such parasite is *Strongyloides stercoralis*, which infects 200 to 300 million persons worldwide and under certain conditions can cause a disseminated hyperinfection that is frequently fatal if untreated (15, 16). The DAF-12 homolog of *S. stercoralis* has 42% sequence similarity with *C. elegans* DAF-12 and a similar affinity for binding DA (10). Previous studies showed that exogenous DA treatment in postfree-living *S. stercoralis* prevents the formation of the iL3 stage (10, 11). Moreover, the most active ligand of DAF-12, Δ7-DA, significantly reduces parasite burdens in mice with an *S. stercoralis* hyperinfection (17). Taken together, these studies suggest that DAF-12 has potential as a therapeutic target for treating *S. stercoralis* parasitism and perhaps parasitism by other nematodes. Thus, characterizing the DAF-12 signaling pathway in *S. stercoralis* is essential to explore this potential.

Significance

Understanding the molecular mechanisms controlling nematode parasite infection is important to developing new therapeutic strategies. The DAF-12 nuclear receptor signaling pathway in free-living nematodes regulates a process known as the dauer diapause. In nematode parasites, this signaling pathway is believed to govern the infectious stage. To investigate this hypothesis, we characterized the orthologous components of DAF-12 and a parasite-specific transcriptional coactivator in the potentially lethal parasite *Strongyloides stercoralis*. Using a CRISPR method developed specifically for *S. stercoralis*, we demonstrate that DAF-12 and its coactivator are required for both the entry into and exit from the infectious stage. These studies further highlight the potential of therapeutically targeting this pathway in *S. stercoralis* and other nematode parasites.

Author contributions: M.C.C., J.B.L., S.A.K., and D.J.M. designed research; M.C.C. and Z.W. performed research; J.B.L., S.A.K., and D.J.M. supervised the project; T.G.J. and X.L. contributed new reagents/analytic tools; M.C.C., Z.W., J.B.L., S.A.K., and D.J.M. analyzed data; and M.C.C., J.B.L., S.A.K., and D.J.M. wrote the paper.

Reviewers: A.A., Max Planck Institute for Biology of Ageing; and D.D.M., Baylor College of Medicine.

The authors declare no competing interest.

[1]To whom correspondence may be addressed. Email: Steven.Kliewer@UTSouthwestern.edu or davo.mango@utsouthwestern.edu.

This article contains supporting information online at https://www.pnas.org/lookup/suppl/doi:10.1073/pnas.2021864118/-/DCSupplemental.

Published February 18, 2021.

As transcription factors, the activities of nuclear hormone receptors like DAF-12 are tuned by coregulators (corepressors and coactivators). Corepressors generally interact with unliganded receptors to repress target gene expression, whereas coactivators typically interact with ligand-bound receptors to stimulate gene expression. In mammals, several dozen nuclear hormone coregulators have been identified and found to be associated with numerous disease states and metabolic disorders (18). In *C. elegans*, the ligand-dependent activity of DAF-12 is governed by one known coregulator, the corepressor DIN-1 (19). The study of this coregulator has added to our understanding of *daf-12* phenotypic complexity and the endocrine signaling network that it regulates. However, interestingly, DIN-1 is not present in *S. stercoralis*, leaving open the question of how the transactivation of DAF-12 is regulated in the parasite.

In this study, we identified a *Strongyloides* parasite-specific DAF-12 coactivator called DAF-12 interacting protein-1 (DIP-1) and investigated the requirement of both the DAF-12 receptor and the coactivator for their roles in regulating the parasite's lifecycle. We find that *S. stercoralis* (Ss)-DAF-12 and Ss-DIP-1 are key factors for *S. stercoralis* to progress to the infectious iL3 stage in its life cycle, and thus represent potential new drug targets to combat *S. stercoralis* infection.

Results

Ss-DAF-12 Is Essential for Development of Infectious-Stage Parasites. We previously showed that Δ7-DA binds and activates the *S. sterocoralis daf-12* gene homolog, Ss-DAF-12, and that premature transactivation of Ss-DAF-12 blocks iL3 development (10, 11). However, the lack of an appropriate experimental system has prevented the study of the direct involvement of Ss-DAF-12 in governing the parasite's biology. Although RNAi has not been effective in *S. stercoralis*, CRISPR-based approaches have been successful (20). To that end, we used CRISPR editing to disrupt the ligand-dependent activation function-2 (AF-2) domain of *Ss-daf-12* with the insertion of a homology-directed repair template that contains a GFP reporter gene under the control of the *Strongyloides ratti* (*Sr*) *eef-1* promoter (Fig. 1*A*). The *Sr-eef-1* promoter drives a high level of reporter expression in *S. stercoralis* that permits selection of CRISPR-targeted F1 progeny (20, 21). The AF-2 domain was targeted because it is required for ligand-dependent coregulator interaction and its mutation in *C. elegans* DAF-12 disrupts activity of this nuclear receptor, resulting in a dauer-defective phenotype (4). Plasmids expressing Cas9, a single-guide RNA (sgRNA) against *Ss-daf-12*, and the homology-directed repair template plasmid were microinjected into the gonads of free-living female worms. These were mated with noninjected free-living males and their progeny screened for reporter expression, phenotypes, and mutant genotypes (*SI Appendix*, Fig. S1). Control worms were injected similarly but without the Cas9 plasmid.

As a secondary negative control, we also targeted the *Ss-unc-22* gene using the same CRISPR protocol (see Fig. 5 below). To confirm transformation of postfree-living larvae with the CRISPR/Cas9 elements, we observed expression of the GFP reporter and subsequently confirmed its insertion into the *daf-12* gene by single-worm PCR. Among GFP^+ worms, single-worm PCR demonstrated that ~80% (38 of 48) showed the correctly targeted insertion, demonstrating the efficacy of CRISPR editing (Fig. 1*B*). Approximately 90% of these worms were heterozygous for the insertion, while the rest were homozygous. In control worms, the progeny of the free-living adults advanced through two larval stages and developmentally arrested as infectious iL3 worms within 7 d (*SI Appendix*, Table S1). In contrast, after 7 d no viable GFP^+ worms (i.e., those that were CRISPR mutants) were observed (*SI Appendix*, Table S1). This finding is consistent with the notion that *Ss-daf-12* mutant worms die before reaching the iL3 stage and provides evidence that *Ss-daf-12* is essential for the development of infective larvae.

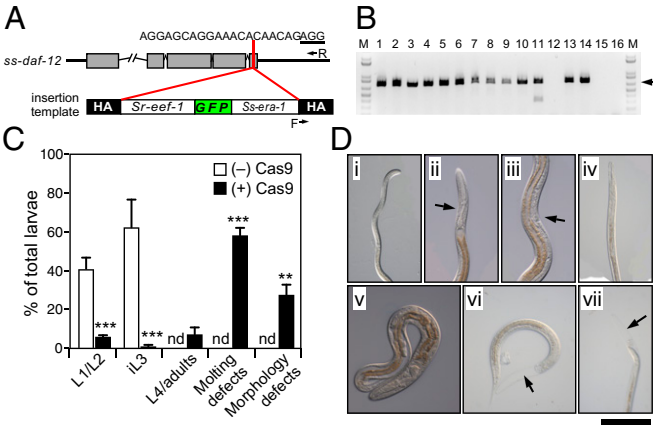

Fig. 1. Ss-DAF-12 is required for iL3 formation. (*A*) *Ss-daf-12* CRISPR targeting vector for homology-directed repair. Red line indicates position of the insertion repair template in the AF-2 domain of the *Ss-daf-12* gene (SSTP_0001172300) and the guide sequence and PAM site (underlined). F, R, forward and reverse primers, respectively; HA, 500-bp homology arms. (*B*) Representative image of single-worm genotyping of F1 generation worms expressing GFP from injected postparasitic free-living females. Single-worm PCR was performed with primers shown in *A* to reveal successful integration (arrowhead indicates 797-bp product) of *Sr-eef-1::GFP* into the target site. (*C*) Quantitation of *Ss-daf-12* CRISPR worms with different phenotypes. Worms injected without (–) the Cas9 plasmid indicate negative controls. Worms that included Cas9 (+) indicate *Ss-daf-12* mutant worms. $^{**}P < 0.001$, $^{***}P < 0.0001$ by two-way ANOVA test comparing (+) Cas9 ($n = 3 \pm$ SD, number of progeny from each experiment tested = 96, 68, 68) to (–) Cas9 ($n = 3 \pm$ SD, number of progeny from each experiment tested = 53, 79, 53); nd, not detected. (*D*) Representative differential interference contrast (DIC) microscopy images from *C* comparing a wild-type iL3 worm (*i*) to CRISPR mutant *Ss-daf-12* worms showing adult-like phenotypes (*ii*, *iii*), body morphology defects (*iv*, *v*), and molting defects (*vi*, *vii*). Arrows show adult-like pharynx structure (*ii*), adult vulva/reproductive organs (*iii*), and defects in cuticle formation (*vi*, *vii*). (Scale bar, 100 μm.)

To further address the timing and requirement of *Ss-daf-12* for iL3 development, we repeated the experiment and collected worms beginning at 3 d after injection when the postfree-living L2 worms are just beginning to transition to the iL3 stage (Fig. 1*C*). At this time point, viable GFP^+ worms were present, but all had defects in body morphology and molting, or had developed to precocious L4/adult-stage worms that had bypassed the arrested iL3 stage (Fig. 1 *C* and *D*). This latter phenotype is similar to that observed in Δ7-DA–treated worms (9–11) and is consistent with the conclusion that at the infectious stage of the lifecycle, Ss-DAF-12 is required for developmental arrest and iL3 formation. Accordingly, some *Ss-daf-12* mutant larvae developed to morphologically fully formed second-generation free-living females (Fig. 1*D*). In *C. elegans*, a similar DAF-12 AF-2 mutation is called dauer-defective; these worms are not able to arrest as third-stage dauer larvae and instead exhibit the mutant phenotypes (4) similar to those observed in the *Ss-daf-12* AF-2 mutation.

Ss-DIP-1 Is a Parasite-Specific DAF-12 Coactivator. Given that *S. stercoralis* lacks any of the known nuclear receptor coregulators, we performed a yeast-two hybrid screen to identify the coregulator that is responsible for Ss-DAF-12 transactivation. We used the Ss-DAF-12 ligand-binding domain (LBD) as bait and screened against proteins from a cDNA library of genes expressed in the postfree-living L1, L2, and iL3 stages. We first confirmed that the Ss-DAF-12 LBD behaves similarly to other nuclear receptors by demonstrating that it can interact with the *C. elegans* cofactor, DIN-1S, in a DA-specific manner (*SI Appendix*, Fig. S2). We then

screened for *S. stercoralis*-specific proteins that interact with Ss-DAF-12. We identified one protein that interacts with Ss-DAF-12 in the presence of Δ7-DA (Fig. 2*A*), which we named Ss-DIP-1, as a candidate coactivator. Interestingly, the screen did not reveal any candidate corepressors. Ss-DIP-1 is a 525-amino acid protein with no readily identifiable functional domains (Fig. 2*B*). Moreover, no genes with significant similarity to *Ss-dip-1* are present in the *C. elegans* (Ce) genome. The only organisms that we found with genes homologous to Ss-DIP-1 were in the parasitic nematode family *Strongyloididae* (*SI Appendix*, Fig. S3), suggesting that this coactivator might have evolved after this family diverged from other nematodes. Consistent with this phylogenetic specificity, Ce-DAF-12, which shares 42% identity in its LBD with Ss-DAF-12, interacted only weakly with Ss-DIP-1 (Fig. 2*A*).

To confirm the interaction between Ss-DAF-12 and Ss-DIP-1, we performed a mammalian two-hybrid assay. To overcome the poor expression of Ss-DAF-12 in mammalian cells, we used a chimeric receptor construct in which the Ce-DAF-12 DNA binding domain (DBD) was fused to the LBD of Ss-DAF-12 (10). The resulting construct (CeSs-DAF-12) was fused to the VP16 transactivation domain and assayed for its interaction with Gal4-Ss-DIP-1 in COS-7 cells. We used SRC-1 (steroid receptor coactivator-1) as a positive control because it is an established mammalian coactivator that interacts with Ce-DAF-12 and Ss-DAF-12 (6, 10). Despite being poorly expressed in mammalian cells (*SI Appendix*, Fig. S4*A*), Gal4-Ss-DIP-1 increased expression of the reporter gene over 30-fold in the presence of Vp16-CeSs-DAF-12 and its ligand, Δ7-DA (*SI Appendix*, Fig. S4*B*). Notably, when the Ss-DIP-1 sequence was codon-optimized for increased expression in mammalian cells (*SI Appendix*, Fig. S4*A*), the ligand-dependent interaction with DAF-12 increased to a level (>200-fold) that was similar to that observed with the SRC-1 control (Fig. 2*C* and *SI Appendix*, Fig. S4*B*). Numerous mammalian coactivators have been shown to interact with nuclear receptors (22, 23). SRC-1, for example, interacts with a broad range of nuclear receptors, including mammalian liver X nuclear receptor (LXR) and retinoid X receptor (RXR), as well as Ce-DAF-12 and Ss-DAF-12 (Fig. 2*C*). In contrast, Ss-DIP-1 coactivated only the DAF-12 receptor from *Strongyloides* spp. In addition to coactivating DAF-12 from *S. stercoralis* (Fig. 2*C*), Ss-DIP-1 from the related species, *Strongyloides ratti*, also markedly enhanced the ligand-dependent activation of DAF-12 (*SI Appendix*, Fig. S5), further demonstrating its unique receptor and species specificity.

We next tested transactivation of Ss-DAF-12 on a luciferase reporter containing the *lit-1* kinase promoter, which is an established DAF-12 target gene with identified DAF-12 binding sites. In the presence of Ss-DIP-1, Ss-DAF-12 transactivated the *lit-1* promoter and Δ7-DA markedly enhanced this activation (Fig. 2*D*), demonstrating that DIP-1 is a functional coactivator of Ss-DAF-12.

Ss-DIP-1/Ss-DAF-12 Interaction Domains. Nuclear receptor coactivators often have a conserved LXXLL motif, which mediates their interactions with nuclear receptors (24). However, Ss-DIP-1 does not have this motif. To identify the region of Ss-DIP-1 that interacts with Ss-DAF-12, we performed mammalian two-hybrid assays with truncation mutants of Ss-DIP-1 (amino acids 1 to 100, 1 to 67, and 1 to 34) and confirmed their expression (*SI Appendix*, Fig. S6). Amino acids 1 to 100 and 1 to 67 interacted with Ss-DAF-12, while amino acids 1 to 34 did not, suggesting that residues 34 to 67 are important for interaction with Ss-DIP-1 (Fig. 3*A*). Inspection of this region revealed a single motif (FPTLL) that is similar to the canonical LXXLL motif. To test the importance of this motif, we individually mutated each of these residues to alanine. F56A, P57A, T58A, and L60A substitutions in Ss-DIP-1 caused modest decreases in its interaction with Ss-DAF-12, while the L59A mutant and F56A/P57A double-mutant caused severe impairment of this interaction (Fig. 3*B*). To further demonstrate the importance of this motif, we substituted the phenylalanine at amino acid 56 with a leucine to convert it from FXXLL to a canonical LXXLL motif. This F56L substitution in Ss-DIP-1 markedly decreased its interaction with Ss-DAF-12 (Fig. 3*C*). These results suggest that in contrast to other coregulators that preferentially mediate their interactions with receptors through LXXLL motifs, the FXXLL motif in Ss-DIP-1 is a specific adaptation for mediating its interaction with Ss-DAF-12.

To further characterize the molecular basis of Ss-DIP-1 coactivation of DAF-12, we investigated the structural features of Ss-DAF-12 responsible for the ligand-dependent interaction. Nuclear receptor LBDs have a conserved tertiary structure composed of a globular domain of α-helices (numbered H1 to H12) arranged in a three-layer "sandwich." The X-ray crystal structure of Ss-DAF-12 has a similar structure and previous structural studies identified several amino acid residues required for ligand binding, including tryptophan-611 (10). Mutation of this residue (W611R) in Ss-DAF-12 abolished receptor transactivation as expected and disrupted the interactions with both Ss-DIP-1 and SRC-1 (Fig. 3*D*). In other nuclear receptors, the AF-2 domain in helix 12 is required for ligand-dependent interaction with coactivators like SRC-1 (25). In Ss-DAF-12 the glutamate (E747) in the AF-2 domain is conserved and, like in other nuclear receptors, forms hydrogen bonds with LXXLL coactivator sequences to form a charge clamp that stabilizes the receptor/coactivator interaction (26). Mutation of this residue (E747Q) in Ss-DAF-12 disrupted the ligand-dependent interaction between Ss-DAF-12 and Ss-DIP-1 (Fig. 3*D*). This result indicates that the AF-2 domain of Ss-DAF-12 mediates binding to Ss-DIP-1 similar to other coactivator–nuclear receptor interactions.

***Ss-dip-1* Expression.** To investigate *Ss-dip-1* expression in *S. stercoralis*, we generated a GFP reporter worm using a *Ss-dip-1p::GFP* expression construct. This construct showed GFP expression in head neurons, the pharynx, and the hypodermis (Fig. 4*A*). Using a *Ss-daf-12p::GFP* construct, we found that *Ss-daf-12* has a similar expression pattern, further supporting the coordinate role of these proteins and their biologically relevant interaction (Fig. 4*B*). We found that expression levels of both *Ss-dip-1* and *Ss-daf-12* reporters increased in the hypodermis at the iL3 stage (Fig. 4*C*).

Ss-DIP-1 Controls iL3 Recovery by Ss-DAF-12. Taken together, these findings support a model in which the entry and exit into the infectious iL3 stage is governed by a DAF-12–dependent gene-expression program similar to what has been observed in *C. elegans* entry and exit from dauer (5). To further test the role of Ss-DIP-1 in governing iL3 reactivation in vivo, we disrupted DIP-1 expression by inserting a *Sr-eef-1p::GFP* construct into the *Ss-dip-1* gene using CRISPR/Cas9-directed homologous recombination and then selected for GFP-expressing mutant *Ss-dip-1* worms (Fig. 5*A* and *SI Appendix*, Table S2). We confirmed *Sr-eef-1p::GFP* insertion by amplifying the surrounding genomic region (Fig. 5*A*). Approximately 80% (45 of 56) of GFP^+ worms showed insertion of the intended gene (Fig. 5*B*). As a negative control, we used *Ss-unc-22* CRISPR worms (20). Disruption of *Ss-dip-1* suppressed developmental activation of *S. stercoralis* iL3 and decreased feeding under host-like culture conditions (in DMEM at 37 °C) (Fig. 5*C*). This result suggests that Ss-DIP-1 is important for reactivation of development once iL3 worms infect their host. We next examined the effect of Δ7-DA treatment in the *Ss-dip-1* mutants. In wild-type worms, Δ7-DA induces iL3 recovery and stimulates worms to initiate feeding as would be expected to occur in favorable conditions upon host infection (10, 11). However, because the Δ7-DA–treated worms are outside of the host without food (an unfavorable condition), they are unable to complete their development and quickly die (Fig. 5*D*),

DEVELOPMENTAL BIOLOGY

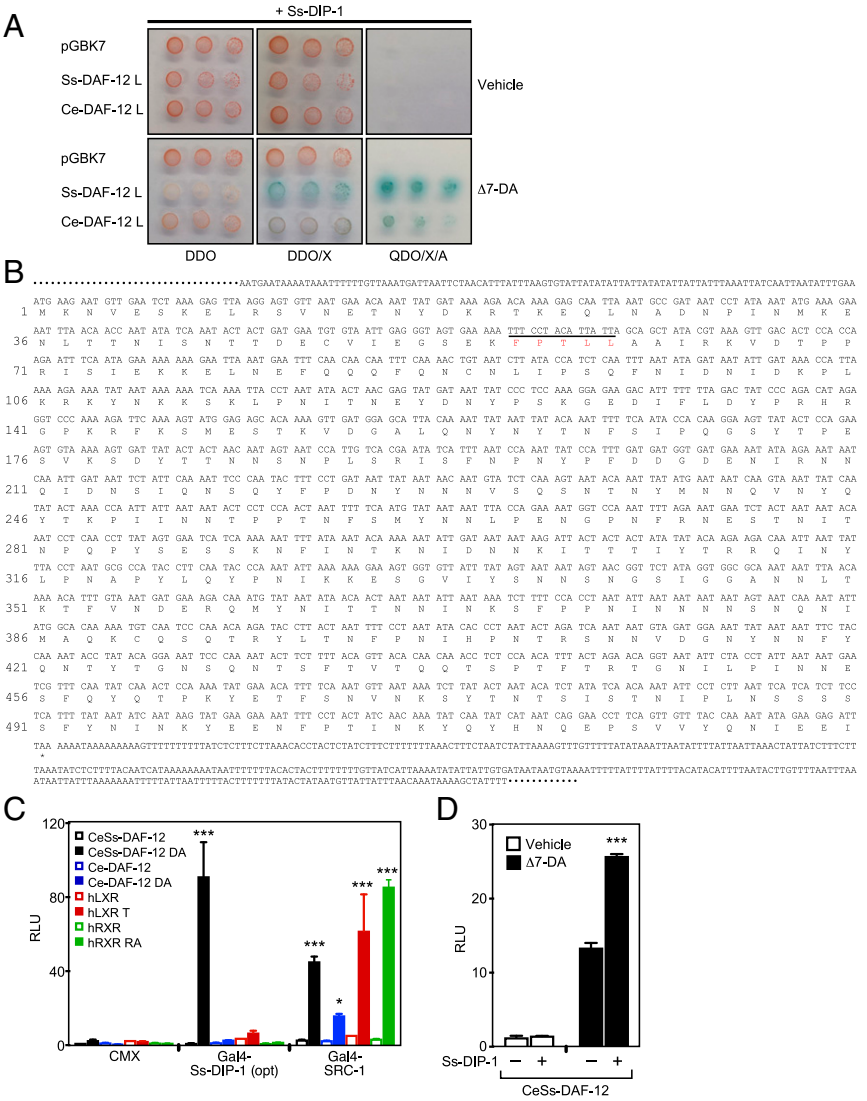

Fig. 2. Ss-DIP-1 is a Ss-DAF-12 coactivator. (*A*) Yeast two-hybrid interaction of Ss-DIP-1 with the ligand binding domain (L) of Ss-DAF-12 or Ce-DAF-12 in the presence of Δ7-DA (1 μM). Serial dilutions of yeast cells were spotted on both permissive (DDO and DDO/X) and selective (QDO/X/A) media and incubated for 3 d at 30 °C. DDO indicate SD/-Leu/-Trp and QDO indicate SD/-Ade/-His/-Leu/-Trp. "X" is X-α-gal and A indicates Aureobasidin A. (*B*) *Ss-dip-1* (SSTP_0000616600) cDNA sequence and predicted protein product. Underline and red lettering indicate position of the FXXLL motif. (*C*) Mammalian two-hybrid interaction of Ss-DIP-1 with various nuclear receptors in COS-7 cells. Agonists used were 1 μM T0901317 (LXR), 10 μM 9-*cis* retinoic acid (RXR), 1 μM Δ7-DA (DAF-12). ***$P <$ 0.0001, and *$P < 0.05$ by two-way ANOVA test comparing agonist to vehicle-treated cells $n = 3 \pm$ SD. (*D*) Ss-DIP-1 increases ligand-dependent transactivation of DAF-12 on a *lit-1* reporter gene in cotransfected SL2 cells. ***$P < 0.0001$ by two-way ANOVA test comparing cells with Ss-DIP-1 to those without Ss-DIP-1 ($n = 3 \pm$ SD).

as has been shown previously (27). Notably, disruption of *Ss-dip-1* resulted in a similar phenotype and decreased parasite mortality (Fig. 5*D*), consistent with the notion that Ss-DIP-1 plays an important role in Δ7-DA–induced iL3 activation.

Finally, we examined genes that are known to be regulated by DAF-12 using qPCR. Previous work showed that *Ss-acs-1*, *Ss-acbp-3*, and *Ss-F28H7.3* are regulated by Δ7-DA (5). Coactivators generally interact with ligand-bound nuclear receptors to stimulate gene expression. Therefore, we hypothesized that Ss-DIP-1 also regulates Ss-DAF-12 target gene expression. As expected, increased expression of *Ss-acs-1*, *Ss-acbp-3*, and *Ss-F28H7.3* genes was abrogated in *Ss-dip-1* CRISPR worms (Fig. 5*E*). These results support the notion that Ss-DIP-1 controls iL3 recovery through the transactivation of Ss-DAF-12. These findings confirm that Ss-DAF-12 is a key switch for parasitic development and that Ss-DIP-1 controls iL3 recovery as a Ss-DAF-12 coactivator.

Discussion

DAF-12 is a hormone-dependent nuclear receptor that is found uniquely in nematodes. In *C. elegans* it is a master transcriptional regulator of the metabolic and developmental program that controls dauer diapause and reproductive maturity (4, 5, 19). In parasitic species, the role of DAF-12 has not been thoroughly investigated but it has been proposed to govern the iL3 stage (8), which is similar to the L3 dauer stage found in free-living species (28). In this study, using newly developed transgenic techniques in the human parasite, *S. stercoralis*, we show that Ss-DAF-12 is a key factor in governing iL3-stage biology, and that this role requires an atypical transcriptional cofactor, Ss-DIP-1.

The discovery of Ss-DIP-1 as a DAF-12–specific coactivator provides an unprecedented understanding of a key molecular mechanism that governs parasite infection. Intriguingly, while Ss-DIP-1 shares features similar to the known canonical nuclear

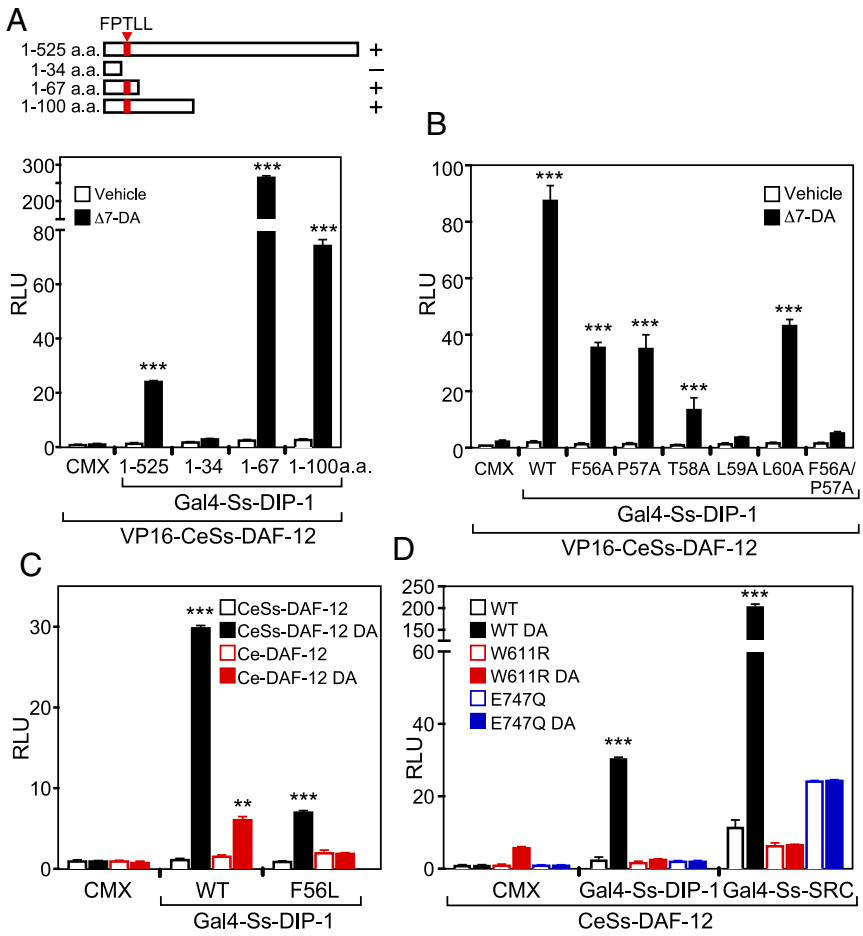

Fig. 3. Ss-DIP-1 and Ss-DAF-12 mutagenesis defines the cofactor/nuclear receptor interaction domains. (*A*) Truncation mutants of Ss-DIP-1 (shown in diagram) were analyzed in a DAF-12 mammalian two-hybrid assay. Red line indicates position of FPTLL motif. (*B*) Effect of Ss-DIP-1 point mutations in the FPTLL motif on the interaction with Ss-DAF-12. (*C*) Effect of the Ss-DIP-1 F56L mutation on DAF-12 interaction. (*D*) Effect of mutations in the Ss-DAF-12 ligand binding pocket (W611R) and AF-2 domain (E747Q) on coactivator interaction. Mammalian two-hybrid cotransfection assays were performed in COS-7 cells in the presence or absence of 1 μM Δ7-DA. $^{**}P < 0.001$, $^{***}P < 0.0001$ by two-way ANOVA test comparing agonist to vehicle treated cells ($n = 3 \pm$ SD).

receptor coactivators, such as its interaction with the AF-2 domain and ligand-dependent transcriptional activity of DAF-12, Ss-DIP-1 has several distinct features that set it apart. First, Ss-DIP-1 has a sui generis receptor interaction that is both receptor- and species-specific. In a search of all known nematode species genomes, Ss-DIP-1 has only been found within the genus *Strongyloides*, and it appears to interact only with the *Strongyloides* DAF-12 receptors. We found that the biochemical basis for this specificity is due to the presence of a receptor interaction domain that contains an atypical FXXLL peptide sequence instead of the canonical LXXLL peptide sequence, in which the phenylalanine is important for DAF-12 interaction. Other nuclear receptors, such as the androgen receptor (AR), have specific coregulators (ARA54, ARA70) in which the leucines of the LXXLL motif have also been replaced by phenylalanine (FXXLF) or tryptophan (WXXLF), and these substitutions are required for their high AR affinity and selectivity (29, 30). A second unique feature of Ss-DIP-1 is that it contains none of the known transactivation regions found in other coactivators, including histone acetyl transferase domains or other transcription factor interactions domains (e.g., p300, CBP). This brings up the intriguing question of how Ss-DIP-1 mediates its transcriptional coactivation function, an area that is the subject of future study.

What might be the reason for the evolution of a species-specific coactivator like Ss-DIP-1? Nematodes as a phylum occupy a wide range of distinct environments. As a nematode-specific transcription factor that governs the dauer-like transition, DAF-12 has been found in all species, both free-living and parasitic. However, each of these species has a unique lifecycle and, thus, the evolution of species-specific coregulators may represent an adaptation to enable an environment-specific developmental pathway. For example, *Strongyloides* and related genera have the unusual ability to complete one or more free-living stages outside of the host before eventually arresting as iL3 infective larvae (*SI Appendix*, Fig. S1). In *S. stercoralis*, we showed that DAF-12 is required in the postfree-living stage for development of iL3 larvae and that its coactivator Ss-DIP-1 is required for the DA-dependent recovery of iL3 larvae. Consistent with this receptor/coactivator interaction, *Ss-dip-1* and *Ss-daf-12* are highly expressed in the iL3 stage based on RNA sequencing (31) and transgenic worm studies (Fig. 4*C*). Similar to dauer larvae in *C. elegans*, DAF-12 is not a transactivator in the iL3 stage, presumably due to the absence of ligand at this stage (*SI Appendix*, Fig. S1). Thus, in the absence of ligand, we propose that Ss-DAF-12 functions as a transcriptional repressor, leading to developmental arrest and formation of infectious iL3 larvae. At this stage, the presence of *Ss-dip-1* would be to anticipate when favorable conditions reoccur (i.e., after host infection) and initiate the synthesis of the DAF-12 ligand, thereby coactivating the transcriptional program that leads to resumption of reproductive development. This hypothesis is supported by the observations that: 1) Activation of DAF-12 by Δ7-DA treatment of postfree-living worms completely prevents

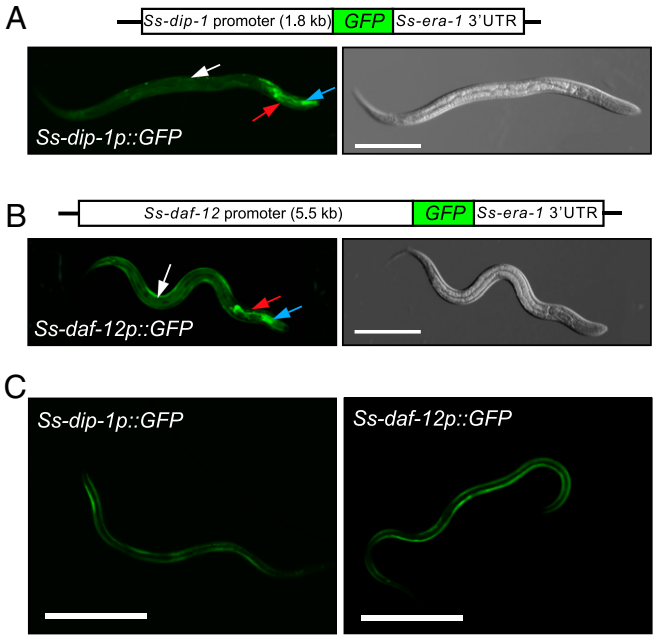

Fig. 4. *Ss-daf-12* and *Ss-dip-1* expression are colocalized. (*A*) *Ss-dip-1p::GFP* expression and (*B*) *Ss-daf-12p::GFP* expression in L2 stage larvae. *Left* and *Right* panels show fluorescent and DIC microscopy images, respectively. White arrow indicates the hypodermis. Blue arrow indicates the pharynx, and red arrow indicates the head neurons. (*C*) *Ss-daf-12* and *Ss-dip-1* promoter-driven expression of the GFP reporter in iL3 larvae. Fluorescence is notable in the hypodermis. (Scale bars,100 μm.)

formation of iL3 larvae, 2) postfree-living worms that lack DAF-12 activity fail to respond to Δ7-DA and never enter the infectious stage, and 3) postfree-living worms that lack Ss-DIP-1 also fail to respond to Δ7-DA.

An interesting nuance of DAF-12 function is that it is both a transcriptional repressor (in the absence of ligand) and a transcriptional activator (in the presence of ligand). Thus, the disruption of DAF-12 function in *S. stercoralis* results in a phenotype similar to the dauer-defective phenotype observed in *C. elegans* in which the loss of the transrepressor function prevents the worms from developmental arrest as iL3 larvae. Instead, many of these larvae progress to adult worms. A similar, albeit less penetrant, phenotype has been observed recently in the related rodent parasite, *S. ratti*, using an RNAi knockdown approach, further validating the evolutionary conservation of this pathway (12). The same phenotype can be achieved by inducing DAF-12 activity in postfree-living wild-type larvae with exogenous Δ7-DA. Both cases result in precocious adult worms that are morphologically abnormal and die within a few days. Notably, in *S. stercoralis* these DA-treated, postfree-living worms are no longer able to establish host infection. These results suggest that *S. stercoralis* needs other host factors in addition to DAF-12 activation to fully resume their developmental program. Alternatively, it is possible that either Ss-DAF-12 or Δ7-DA may have additional roles in other stages of the life cycle. These results raise several questions, including the identity of the endogenous DAF-12 ligand from parasitic nematodes and when and how it is synthesized. It may be that like *C. elegans*, Ss-DAF-12 is important for hormone-mediated developmental timing regulation by heterochronic genes (e.g., *let-7*-family miRNAs) in *S. sterocoralis* (32, 33).

In summary, the discovery of DIP-1 as a parasite-specific, DAF-12-specific coactivator provides a unique understanding of a key molecular mechanism that governs parasite infection. Our work also advances an understanding of the mechanisms that allow nuclear receptors to fine-tune their transcriptional responses.

Materials and Methods

Yeast Two-Hybrid Screening. We performed yeast two-hybrid screening using the MATCHMAKER Gold yeast two-hybrid system (Clontech), following protocols provided by the manufacturer. Briefly, bait vectors were transformed into yeast strain Y2HGold (MATα, trp1-901, leu2-3, 112, ura3-52, his3-200,

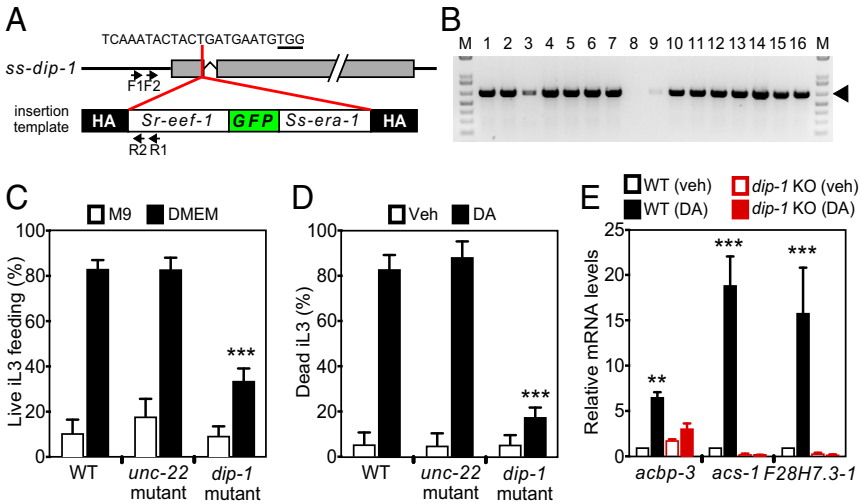

Fig. 5. Ss-DIP-1 controls iL3 recovery. (*A*) CRISPR target site and strategy for homology-directed disruption of *Ss-dip-1*. Red line indicates position of the insertion repair template and guide sequence and PAM site (underlined). Position of forward (F) and reverse (R) primers are shown. (*B*) Representative image of single-worm genotyping. Nested primers in *A* were used to amplify successful integration of *Sr-eef-1::GFP* into the target site. PCR product size for primary PCR with F1 and R1 primers is 884 bp. PCR product size for the nested PCR with F2 and R2 primers is 688 bp (arrowhead). (*C*) Frequency of iL3 feeding in *Ss-dip-1* knockout (KO) versus wild-type (WT) and *Ss-unc-22* KO control worms. Worms were induced to start feeding by placing in DMEM media. ***$P <$ 0.0001 by two-way ANOVA test comparing WT DMEM to *Ss-dip-1* DMEM ($n = 4 \pm$ SD). See *SI Appendix*, Table S3 for number of animals tested, (*D*) *Ss-dip-1* mutant worms show a decreased response to 1 μM Δ7-DA as assayed by iL3 mortality. ***$P < 0.0001$ by two-way ANOVA test comparing Δ7-DA-treated WT to *Ss-dip-1* mutant worms ($n = 5 \pm$ SD). See *SI Appendix*, Table S3 for number of animals tested. (*E*) *Ss-daf-12* target gene expression determined by qPCR. *S. stercoralis* iL3 were treated with or without 400 nM Δ7-DA. **$P < 0.001$, ***$P < 0.0001$ by two-way ANOVA test comparing Δ7-DA to vehicle treated worms ($n = 3 \pm$ SD).

gal4Δ, gal80Δ, LYS2::GAL1UAS–Gal1TATA–His3, GAL2UAS–Gal2TATA–Ade2, URA3::MEL1UAS–Mel1TATA, AUR1-C MEL1). Variable length *Ce-daf-12* and *Ss-daf-12* cDNA fragments were cloned into pGBKT7 vector. Full-length (FL) indicates amino acids 1 to 754; hinge and ligand binding domains (HL) indicates amino acids 240 to 754 (Ce-DAF-12) or 184 to 754 (Ss-DAF-12); and ligand binding domain (L) indicates amino acids 502 to 754 (Ce-DAF-12) or 513 to 754 (Ss-DAF-12). For the preys, we used the "Mate & Plate" Library system and followed the manufacture's protocol (Takara Bio USA, Inc., Mountain View, CA). *S. stercoralis* iL3 cDNA library was cloned into the *pGADT7* vector and transformed into the yeast strainY187 (MATα, ura3-52, his3-200, ade2-101, trp1-901, leu2-3, 112, gal4Δ, gal80Δ, met–, URA3::GAL1UAS–Gal1TATA–LacZ, MEL1). For selection, SD/-Leu/-Trp/X-α-gal/AbA (Aureobasidin A) plates were used. SD/-Leu/-Trp selects diploids containing pGBKT7 and pGADT7. X-α-gal/AbA was used to select for protein–protein interaction. Approximately 8 million colonies were screened; three colonies were identified as not false positives, one of which was found to be DIP-1. Selected colonies were verified by growth on SD/-Ade/-His/-Leu/-Trp/X-α-gal/AbA minimal plates.

Cell Culture and Reporter Assay. For the mammalian two-hybrid assay, COS-7 cells were maintained in DMEM containing 10% fetal bovine serum, 2 mM glutamine, 100 units/mL penicillin, and 100 μg/mL streptomycin in 5% CO_2 at 37 °C. COS-7 cells were transfected in 96-well plates using 50 ng of luciferase reporter, 10 ng CMX-*Renilla* luciferase reporter, 15-ng nuclear receptor expression plasmids (VP16-Ce-DAF-12, VP16-CeSs-DAF-12, VP16-hRXR and VP16-hLXR), and 15-ng empty vector or cofactor expression plasmids (GAL4-Ss-DIP-1, GAL4-SRC), as previously described (10). For DIP-1 truncation constructs, the *Ss-dip-1* cDNA encoding amino acids 1 to 525, 1 to 100, 1 to 67, and 1 to 34 were cloned into the CMX-GAL4 expression vector for use in the mammalian two-hybrid assay. Ethanol (vehicle) or indicated compounds were added to each well 8-h posttransfection, incubated for 16 h, and cells were then harvested for dual luciferase assay. Sr-DIP-1 (SRAE_X000054200) was identified with TBLASTN to search the *S. ratti* genome in WormBase ParaSite using Ss-DIP-1. Ss-DIP-1 and Sr-DIP-1 cDNAs were codon-optimized and purchased from Integrated DNA Technologies (https://www.idtdna.com/pages/tools/codon-optimization-tool?returnurl=%2FCodonOpt). Schneider's *Drosophila* Line 2 (SL2) cells were maintained in Schneider's *Drosophila* medium with 10% heat-inactivated fetal bovine serum at 23 °C. Cells were transfected with luciferase reporter (*lit-1* kinase promoter), pAc5.1-β-galactosidase reporter, nuclear receptor expression plasmids, and empty vector or cofactor expression plasmids. Data represent the mean ± SD from triplicate assays and were plotted by using Graphpad software.

***S. stercoralis* Culture.** *S. stercoralis* was maintained in purpose-bred, prednisone-treated mix-breed dogs, as described previously (34) according to protocol APN 2016-101500 approved by the University of Texas Southwestern Medical Center Institutional Animal Care and Use Committee (IACUC). All IACUC protocols, as well as routine husbandry care of the animals, were conducted in strict accordance with the *Guide for the Care and Use of Laboratory Animals* of the National Institutes of Health (35).

CRISPR. The CRISPR method was based on a previously described protocol (20) using the Cas9 vector pPV540. To find PAM (protospacer adjacent motif) sites, we used the benchling website (https://www.benchling.com/). The sgRNA expression vectors for targeting *Ss-dip-1* and *Ss-daf-12* were modified from pML60, which was a gift from Elissa A. Hallem (University of California Los Angeles, Los Angeles, CA). pAJ50 was included as an injection marker. For the homologous repair template, 500-bp homology arms flanking *Ss-dip-1* and *Ss-daf-12* sites were cloned with *Sr-eef-1p::GFP::era* from Ppv529. Injection mixes contained 60 ng/μL sgRNA expression vector, 20 ng/μL repair template, and 20 ng/μL pPV540. Negative control (-Cas9) mixes lacked the pPV540 Cas9 vector or included *Ss-unc-22* injection mixes that contained 60 ng/μL pML60 and 20 ng/μL pPV540. Postparasitic free-living *S. stercoralis* L1 larvae were collected from dog feces and cultured at 22 °C, as described previously (34) to acquire free-living adults for CRISPR targeting (*SI Appendix*, Fig. S1). Fifty adult females were injected with the CRISPR mixes following standard microinjection techniques established for *C. elegans* (36). Injected females were then placed with adult males in fecal cultures, as described previously (20). The F1 progenies from these matings were collected at 3 or 7 d after injection and placed on NGM plates and screened for GFP expression and phenotypic evaluation using a Leica M165 FC microscope. Insertion of the repair template was checked by single worm PCR genotyping. Approximately 90% of the worms that had the correct inserts were heterozygous for the mutation. PCR primers are listed in *SI Appendix*, Table S4.

***S. sterocoralis* iL3 Reactivation and Feeding Assay.** This assay was performed as previously described with small modifications (11). Worms at the iL3 stage were isolated by the Baermann technique and washed with water twice and incubated with either M9 or DMEM buffer. DMEM is known to stimulate feeding in iL3 worms (37). Each condition (M9 and DMEM) used ~20 iL3 worms in 100 μL in each well and incubated at 37 °C in 5% CO_2 in air for 21 h. Then, 2 μL of FITC (CAS 3326-32-7; Sigma) dissolved in N,*N*-dimethylformamide (DMF) (CAS 68-12-2; Sigma) was added at 20 mg/mL and incubated for 3 h. After 24-h incubation, iL3 worms were collected and washed five times with M9 buffer. Only live iL3 (indicated by movement) with FITC in the pharynx were scored as "positive" for feeding. Three biological replicates were performed. For stimulation of feeding with Δ7-DA treatment, 1 μM Δ7-DA in M9 buffer was used and incubated at 37 °C in 5% CO_2 in for 24 h. Lack of movement was used to score dead worms.

qRT-PCR. RNA was isolated using an individual worm RNA extraction method (38). Briefly, 20 iL3 were transferred into 10 μL worm lysis buffer (5 mM Tris pH 8.0, 0.5% Triton X-100, 0.5% Tween 20, 0.25 mM EDTA and 1 mg/mL proteinase K) in 0.2-mL PCR tubes. The tubes were incubated at 65 °C for 10 min, then 85 °C for 1 min, and then cooled on ice. The worm lysate was used for cDNA synthesis. cDNA was preamplified (TaqMan preAmp Master Mix, Thermo Fisher) before being analyzed by qPCR. Relative mRNA levels were normalized to 18S ribosomal RNA levels. Data are presented as fold-changes of relative mRNA levels in Δ7-DA versus vehicle-treated worms.

Transgene Construction. To generate the *Ss-dip-1p::GFP* construct, 1.8 kb of the *Ss-dip-1* promoter upstream of the predicted *Ss-dip-1* gene was amplified and cloned with *GFP::era-1 3′UTR* from the pPV529 vector. Primer sequences are listed in *SI Appendix*, Table S1. For *Ss-daf-12p::GFP*, 5.5 kb of the *Ss-daf-12* promoter upstream of the gene amplified and cloned with *GFP::era-1 3′UTR* from pPV529. Sequences were obtained from the Wormbase Parasite website (https://parasite.wormbase.org/index.html). To generate transgenic progenies, these plasmids (50 ng/μL) were microinjected with RFP (pAJ50) injection markers (50 ng/μL).

Statistical Analysis. For all experiments, two-way ANOVA analysis was used for multigroup analyses and plots were created with Prism v8 (GraphPad Software). Statistical probabilities $P < 0.05$ were considered significant.

Data Availability. All study data are included in the article and supporting information.

ACKNOWLEDGMENTS. We thank members of the J.B.L. and D.J.M.–S.A.K. laboratories for comments and technical assistance and Dr. Elissa A. Hallem for the pML60 vector. This work was supported by NIH Grants R33 AI105856 (to J.B.L., S.A.K., and D.J.M.) and R01 AI050668 (to J.B.L.); Robert A. Welch Foundation Grants I-1558 (to S.A.K.) and I-1275 (to D.J.M.); and the Howard Hughes Medical Institute (D.J.M.).

1. P. J. Hotez, J. R. Herricks, Helminth elimination in the pursuit of sustainable development goals: A "worm index" for human development. *Plos Neglect. Trop Dis.* **9** e0003618 (2015).
2. R. M. Kaplan, Drug resistance in nematodes of veterinary importance: A status report. *Trends Parasitol.* **20**, 477–481 (2004).
3. H. Rose *et al*., Widespread anthelmintic resistance in European farmed ruminants: A systematic review. *Vet. Rec.* **176**, 546 (2015).
4. A. Antebi, W. H. Yeh, D. Tait, E. M. Hedgecock, D. L. Riddle, *daf-12* encodes a nuclear receptor that regulates the dauer diapause and developmental age in *C. elegans*. *Genes Dev.* **14**, 1512–1527 (2000).
5. Z. Wang *et al*., The nuclear receptor DAF-12 regulates nutrient metabolism and reproductive growth in nematodes. *PLoS Genet.* **11**, e1005027 (2015).
6. D. L. Motola *et al*., Identification of ligands for DAF-12 that govern dauer formation and reproduction in *C. elegans*. *Cell* **124**, 1209–1223 (2006).
7. P. Mahanti *et al*., Comparative metabolomics reveals endogenous ligands of DAF-12, a nuclear hormone receptor, regulating *C. elegans* development and lifespan. *Cell Metab.* **19**, 73–83 (2014).
8. Z. Wang, N. E. Schaffer, S. A. Kliewer, D. J. Mangelsdorf, Nuclear receptors: Emerging drug targets for parasitic diseases. *J. Clin. Invest.* **127**, 1165–1171 (2017).
9. A. Ogawa, A. Streit, A. Antebi, R. J. Sommer, A conserved endocrine mechanism controls the formation of dauer and infective larvae in nematodes. *Curr. Biol.* **19**, 67–71 (2009).
10. Z. Wang *et al*., Identification of the nuclear receptor DAF-12 as a therapeutic target in parasitic nematodes. *Proc. Natl. Acad. Sci. U.S.A.* **106**, 9138–9143 (2009).
11. M. M. Y. Albarqi *et al*., Regulation of life cycle checkpoints and developmental activation of infective larvae in *Strongyloides stercoralis* by dafachronic acid. *PLoS Pathog.* **12**, e1005358 (2016).
12. A. Dulovic, A. Streit, RNAi-mediated knockdown of *daf-12* in the model parasitic nematode *Strongyloides ratti*. *PLoS Pathog.* **15**, e1007705 (2019).

13. G. Ma *et al*., Dafachronic acid promotes larval development in *Haemonchus contortus* by modulating dauer signalling and lipid metabolism. *PLoS Pathog.* **15**, e1007960 (2019).
14. K. O. Ayoade *et al*., Dafachronic acid and temperature regulate canonical dauer pathways during *Nippostrongylus brasiliensis* infectious larvae activation. *Parasit. Vectors* **13**, 162 (2020).
15. M. J. Taylor, T. A. Garrard, F. J. O'Donahoo, K. E. Ross, Human strongyloidiasis: Identifying knowledge gaps, with emphasis on environmental control. *Res. Rep. Trop. Med.* **5**, 55–63 (2014).
16. M. Beknazarova, H. Whiley, K. Ross, Strongyloidiasis: A disease of socioeconomic disadvantage. *Int. J. Environ. Res. Public Health* **13**, 517 (2016).
17. J. B. Patton *et al*., Methylprednisolone acetate induces, and Δ7-dafachronic acid suppresses, *Strongyloides stercoralis* hyperinfection in NSG mice. *Proc. Natl. Acad. Sci. U.S.A.* **115**, 204–209 (2018).
18. D. M. Lonard, R. B. Lanz, B. W. O'Malley, Nuclear receptor coregulators and human disease. *Endocr. Rev.* **28**, 575–587 (2007).
19. A. H. Ludewig *et al*., A novel nuclear receptor/coregulator complex controls *C. elegans* lipid metabolism, larval development, and aging. *Genes Dev.* **18**, 2120–2133 (2004).
20. S. S. Gang *et al*., Targeted mutagenesis in a human-parasitic nematode. *PLoS Pathog.* **13**, e1006675 (2017).
21. H. Shao, X. Li, J. B. Lok, Heritable genetic transformation of *Strongyloides stercoralis* by microinjection of plasmid DNA constructs into the male germline. *Int. J. Parasitol.* **47**, 511–515 (2017).
22. S. A. Oñate, S. Y. Tsai, M. J. Tsai, B. W. O'Malley, Sequence and characterization of a coactivator for the steroid hormone receptor superfamily. *Science* **270**, 1354–1357 (1995).
23. X. Gan *et al*., Dual mechanisms of ABCA1 regulation by geranylgeranyl pyrophosphate. *J. Biol. Chem.* **276**, 48702–48708 (2001).
24. R. S. Savkur, T. P. Burris, The coactivator LXXLL nuclear receptor recognition motif. *J. Pept. Res.* **63**, 207–212 (2004).
25. S. Westin *et al*., Interactions controlling the assembly of nuclear-receptor heterodimers and co-activators. *Nature* **395**, 199–202 (1998).
26. W. Bourguet, P. Germain, H. Gronemeyer, Nuclear receptor ligand-binding domains: Three-dimensional structures, molecular interactions and pharmacological implications. *Trends Pharmacol. Sci.* **21**, 381–388 (2000).
27. J. D. Stoltzfus, S. M. Bart, J. B. Lok, cGMP and NHR signaling co-regulate expression of insulin-like peptides and developmental activation of infective larvae in *Strongyloides stercoralis*. *PLoS Pathog.* **10**, e1004235 (2014).
28. M. Crook, The dauer hypothesis and the evolution of parasitism: 20 years on and still going strong. *Int. J. Parasitol.* **44**, 1–8 (2014).
29. B. He, J. T. Minges, L. W. Lee, E. M. Wilson, The FXXLF motif mediates androgen receptor-specific interactions with coregulators. *J. Biol. Chem.* **277**, 10226–10235 (2002).
30. D. J. van de Wijngaart *et al*., Novel FXXFF and FXXMF motifs in androgen receptor cofactors mediate high affinity and specific interactions with the ligand-binding domain. *J. Biol. Chem.* **281**, 19407–19416 (2006).
31. J. D. Stoltzfus, S. Minot, M. Berriman, T. J. Nolan, J. B. Lok, RNAseq analysis of the parasitic nematode *Strongyloides stercoralis* reveals divergent regulation of canonical dauer pathways. *PLoS Negl. Trop. Dis.* **6**, e1854 (2012).
32. A. Bethke, N. Fielenbach, Z. Wang, D. J. Mangelsdorf, A. Antebi, Nuclear hormone receptor regulation of microRNAs controls developmental progression. *Science* **324**, 95–98 (2009).
33. C. M. Hammell, X. Karp, V. Ambros, A feedback circuit involving *let-7*-family miRNAs and DAF-12 integrates environmental signals and developmental timing in *Caenorhabditis elegans*. *Proc. Natl. Acad. Sci. U.S.A.* **106**, 18668–18673 (2009).
34. J. B. Lok, *Strongyloides stercoralis*: A model for translational research on parasitic nematode biology. WormBook, The C. elegans Research Community, Ed. (Wormbook, 2007). http://www.wormbook.org/chapters/www_strongyloides/strongyloides.html. Accessed 11 February 2021.
35. National Research Council, *Guide for the Care and Use of Laboratory Animals* (National Academies Press, Washington, DC, ed. 8, 2011).
36. T. Evans, Ed. "Transformation and microinjection" in *WormBook*, The *C. elegans* Research Community, Eds. (Wormbook, 2006), 10.1895/wormbook.1.108.1.
37. F. T. Ashton, X. Zhu, R. Boston, J. B. Lok, G. A. Schad, *Strongyloides stercoralis*: Amphidial neuron pair ASJ triggers significant resumption of development by infective larvae under host-mimicking in vitro conditions. *Exp. Parasitol.* **115**, 92–97 (2007).
38. K. Ly, S. J. Reid, R. G. Snell, Rapid RNA analysis of individual *Caenorhabditis elegans*. *MethodsX* **2**, 59–63 (2015).